

Shape and Failure Control of Composite Laminates using Piezoelectric Actuators

Zeaid Hasan*¹

¹Texas A&M University, College Station, Texas

*Corresponding author: zeadnws@gmail.com

Abstract: Smart materials are candidates for efficient shape control of high precision surfaces such as antenna reflectors and optical mirrors and there exist several different types of piezoelectric materials such as Lead Zirconate Titanate (PZT), Microfiber Composites (MFCs), and Active fiber composites (AFCs) which could be used for this purpose. The present work focuses on the use of piezoelectric materials for shape control of composite laminates by using several different types of actuators using the commercial finite element software COMSOL. Due to the high stress concentration between the interface of the host structure and the active part; embedded actuators are used as an alternative for the patched design where the active part is incorporated into one of the layers of the composite beam during the manufacturing process, thus, eliminating the stress concentration while obtaining similar actuation values. A control algorithm is also proposed based on the classical lamination theory (CLT) for predicting the failure load and mode of a composite laminate under uniaxial loading, and by using active materials, a counter electric potential could be applied to prevent failure from occurring.

Keywords: Piezoelectric, Composite Laminates, Actuators

1. Introduction

Human civilization has been influenced significantly by materials technology and most periods of technological development have been linked to changes in the use of materials (e.g the stone, bronze and iron ages). In new generations the driving force for technological changes has led to a new family of engineered materials and structures exhibiting multifunctional capabilities which are naturally seen in biological systems, leading to a new era of smart materials. The structures with surface mounted or embedded sensors and actuators that have the capability to sense and take corrective action are referred to as smart structures [1]. These types of system find

applications in aircraft wings, helicopter rotors and automobiles. One of the main motivations behind the vast attentions on smart materials and structures in recent years is its ability to incorporate active materials into the structure as sensors and actuators so that it could be used to monitor the integrity/health of the structure to enable a structure to change its shape or its material properties [2], or to control vibration [3]. These lead to improving performance and service life of the system.

In shape control, one intends to specify the spatial distribution, or the shape, of an actuating control unit, such that the displacement field of a structure distorted from its original shape eventually vanishes, or such that the structure follows some desired field of path. The disturbances that distort the shape of structures may be transient (dynamic), or they may be slowly varying in time (quasi-/static). Shape control represents a branch of structural engineering that is closely related to control engineering.

Many researchers can be recognized for their unique work in shape control using piezoelectric material, [4-5] have several contributions in shape control using piezoelectric layers, where these layers were developed and experimentally implemented so as to excite a specific structural mode, or to measure a specific modal content of the structural vibrations excited by external disturbances. The changes in shapes of fiber-reinforced composite beams, plates, and shells affected by embedded piezoelectric actuators were investigated analytically by [2]. The distributed structural control of elastic shell continua using spatially distributed modal piezoelectric actuators was proposed, and some generic distributed feedback algorithms with spatial feedback functions were formulated [6]. Finite difference modeling and shape control of piezoelectric actuator embedded elastic plates was also considered [7], estimating optimal actuation voltages to match the deflection of the plate to a desired deflection.

The mechanics of smart material systems involves coupling between electric, magnetic, thermal, and mechanical effects. In addition to this coupling, it may be necessary to account for geometric and material nonlinearities. An example is the use of an electromechanical transducer that is characterized by five important properties including the resonant frequency, acoustic impedance, mechanical damping coefficient, electromechanical coupling coefficient and the electric impedance. If nonlinear electroelastic equations are included in the model, some or all of these properties can be tuned; for instance, in an electrostrictive material, the electromechanical coupling coefficient can be tuned with a bias field [1]. In order to tune the first fundamental resonant frequency of the transducer, thin rubber layers are introduced in a multi-layer PZT laminate [8]. The thin rubber layers necessitate the use of nonlinear elastic relations, such nonlinearity in electroelastic formulations was considered by [9], also, a two-dimensional theory of electrostriction was considered by [10] and solved a simplified boundary value problem using complex potentials.

2. Piezoelectric Materials

The phenomenon of piezoelectricity was discovered in 1880 by the Jacques and Pierre Curie brothers. They found out that when a mechanical stress was applied on crystals such as tourmaline, topaz, quartz, Rochelle salt and cane sugar, electrical charges appeared with opposite signs on opposite surfaces and these charges were proportional to the stress.

Significant impetus has been generated by the discovery of piezoelectricity in polycrystalline ceramic materials like barium-titanate (BT) in the 1940's and lead-zirconate-titanate (PZT) in the 1950's; the latter still dominates transducer applications. Semicrystalline piezoelectric polymers on the basis of polyvinylidene fluoride (PVDF) usually in the form of thin films have been available since the late 1960's. Newer development tendencies are directed towards the improvement of PZT ceramics by doping them with additional components such as La₂O₃ or producing artificial piezoelectric monocrystals. Piezoelectric materials exhibit electromechanical coupling, which is useful for the design of

devices for sensing and actuation. The coupling is exhibited in the fact that piezoelectric materials produce an electrical displacement when a mechanical stress is applied which is termed the direct piezoelectric effect and can also produce mechanical strain under the application of an electric field which is known as the converse piezoelectric effect.

The linear constitutive relations for the k^{th} orthotropic lamina in the principal material coordinates of a lamina including electrical effects are

$$\begin{aligned} \begin{Bmatrix} \sigma_1 \\ \sigma_2 \\ \sigma_6 \end{Bmatrix}^k &= \begin{bmatrix} Q_{11} & Q_{12} & 0 \\ Q_{21} & Q_{22} & 0 \\ 0 & 0 & Q_{66} \end{bmatrix}^k \begin{Bmatrix} \varepsilon_1 \\ \varepsilon_2 \\ \varepsilon_6 \end{Bmatrix} \\ - \begin{bmatrix} 0 & 0 & e_{31} \\ 0 & 0 & e_{32} \\ 0 & 0 & 0 \end{bmatrix}^k &\begin{Bmatrix} E_1 \\ E_2 \\ E_3 \end{Bmatrix}^k \end{aligned} \quad (1)$$

where Q_{ij}^k is the plane stress-reduced stiffness, e_{ij}^k is the piezoelectric moduli of the k^{th} lamina, σ_i is the stress vector, ε_i is the strain vector and E_i is the electric field vector referred to the material coordinate system (x_1, x_2, x_3), respectively. For layers other than piezoelectric layers, the part containing the piezoelectric moduli e_{ij}^k should be neglected.

The piezoelectric stiffnesses are known in terms of the dielectric constants and elastic stiffnesses as

$$\begin{bmatrix} 0 & 0 & e_{31} \\ 0 & 0 & e_{32} \\ 0 & 0 & 0 \end{bmatrix}^k = \begin{bmatrix} 0 & 0 & d_{31} \\ 0 & 0 & d_{32} \\ 0 & 0 & 0 \end{bmatrix}^k \begin{bmatrix} Q_{11} & Q_{12} & 0 \\ Q_{21} & Q_{22} & 0 \\ 0 & 0 & Q_{66} \end{bmatrix}^k \quad (2)$$

Since the laminate is made of several orthotropic layers, with their material axes oriented arbitrarily with respect to the laminate coordinates, the constitutive equations of each layer must be transformed to the laminate coordinates x, y, z . The transformed stress-strain relations relate the stresses $\sigma_{xx}, \sigma_{yy}, \sigma_{xy}$ to the strains $\varepsilon_{xx}, \varepsilon_{yy}, \gamma_{xy}$ and components of the electric displacement vector E_x, E_y, E_z in the

laminate coordinates

$$\begin{Bmatrix} \sigma_{xx} \\ \sigma_{yy} \\ \sigma_{xy} \end{Bmatrix}^k = \begin{bmatrix} \bar{Q}_{11} & \bar{Q}_{12} & \bar{Q}_{13} \\ \bar{Q}_{21} & \bar{Q}_{22} & \bar{Q}_{23} \\ \bar{Q}_{61} & \bar{Q}_{62} & \bar{Q}_{66} \end{bmatrix}^k \begin{Bmatrix} \varepsilon_{xx} \\ \varepsilon_{yy} \\ \gamma_{xy} \end{Bmatrix} \quad (3)$$

$$- \begin{bmatrix} 0 & 0 & \bar{e}_{31} \\ 0 & 0 & \bar{e}_{32} \\ 0 & 0 & \bar{e}_{36} \end{bmatrix}^k \begin{Bmatrix} E_x \\ E_y \\ E_z \end{Bmatrix}^k$$

Because of the discontinuous variation of stresses from layer to layer, it is more convenient to deal with the integrated effect of these stresses on the laminate. Thus, we seek expressions relating forces and moments to laminate deformation. The expressions for the resultant forces and moments related to the displacement gradients and electric fields are given as follows

$$\begin{Bmatrix} N_x \\ N_y \\ N_{xy} \end{Bmatrix} = \begin{bmatrix} A_{11} & A_{12} & A_{16} \\ A_{21} & A_{22} & A_{26} \\ A_{16} & A_{26} & A_{66} \end{bmatrix} \left\{ \begin{array}{l} \frac{\partial u_0}{\partial x} + \frac{1}{2} \left(\frac{\partial w_0}{\partial x} \right)^2 \\ \frac{\partial v_0}{\partial y} + \frac{1}{2} \left(\frac{\partial w_0}{\partial y} \right)^2 \\ \frac{\partial u_0}{\partial y} + \frac{\partial v_0}{\partial x} + \frac{\partial w_0}{\partial x} \frac{\partial w_0}{\partial y} \end{array} \right\}$$

$$- \begin{bmatrix} B_{11} & B_{12} & B_{16} \\ B_{21} & B_{22} & B_{26} \\ B_{16} & B_{26} & B_{66} \end{bmatrix} \left\{ \begin{array}{l} \frac{\partial^2 w_0}{\partial x^2} \\ \frac{\partial^2 w_0}{\partial y^2} \\ 2 \frac{\partial^2 w_0}{\partial x \partial y} \end{array} \right\} - \begin{Bmatrix} A_1^p \\ A_2^p \\ A_6^p \end{Bmatrix}$$

$$\begin{Bmatrix} M_x \\ M_y \\ M_{xy} \end{Bmatrix} = \begin{bmatrix} B_{11} & B_{12} & B_{16} \\ B_{21} & B_{22} & B_{26} \\ B_{16} & B_{26} & B_{66} \end{bmatrix} \left\{ \begin{array}{l} \frac{\partial u_0}{\partial x} + \frac{1}{2} \left(\frac{\partial w_0}{\partial x} \right)^2 \\ \frac{\partial v_0}{\partial y} + \frac{1}{2} \left(\frac{\partial w_0}{\partial y} \right)^2 \\ \frac{\partial u_0}{\partial y} + \frac{\partial v_0}{\partial x} + \frac{\partial w_0}{\partial x} \frac{\partial w_0}{\partial y} \end{array} \right\}$$

$$- \begin{bmatrix} D_{11} & D_{12} & D_{16} \\ D_{21} & D_{22} & D_{26} \\ D_{16} & D_{26} & D_{66} \end{bmatrix} \left\{ \begin{array}{l} \frac{\partial^2 w_0}{\partial x^2} \\ \frac{\partial^2 w_0}{\partial y^2} \\ 2 \frac{\partial^2 w_0}{\partial x \partial y} \end{array} \right\} - \begin{Bmatrix} B_1^p \\ B_2^p \\ B_6^p \end{Bmatrix}$$

The A, B, and D matrices are called the extensional, coupling, and bending stiffness matrices, respectively. Assuming that the electric fields vary linearly within k^{th} layer; the piezoelectric stiffnesses are defined as [11]

$$A_i^p = \frac{1}{2} \sum_{k=1}^{Na} \sum_{j=1,2,6} \bar{Q}_{ij}^k \bar{d}_{3j}^k (E_1^k + E_1^k) h_k \quad (4)$$

$$d_{3j}^k$$

$$B_i^p = \frac{1}{6} \sum_{k=1}^{Na} \sum_{j=1,2,6} \bar{Q}_{ij}^k \bar{d}_{3j}^k [E_1^k (h_k + 3z_k) + E_2^k (2h_k + 3z_k)] h_k \quad (5)$$

Where Na is the number of actuator layers and the electric field E is defined as

$$E_1^k = E_2^k = \frac{V_k}{h_k} \quad (6)$$

Where V_k is the applied voltage across the k^{th} layer and h_k is the thickness of the layer. Detailed analysis can be found in [11].

3. Piezoelectric Fiber Composites

In order to improve the use of piezoelectric materials in structural applications as sensors and actuators, piezoelectric materials are integrated into composites which allow for improvement of their constitutive properties as well as of failure behavior and consequently for an extension of the application in use. The challenge of modeling these types of materials in structural applications has attracted wide attention in recent years due to their advantages in several applications which we will discuss in the next subsections

3.1 Active Fiber Composite (AFC)

AFC actuators consist of unidirectional, aligned piezoelectric fibers, a resin matrix system, and interdigital electrodes, as shown in

Figure 1, a. The advantages over monolithic piezoceramic actuators include higher planar actuation strains, tailorable directional actuation, robustness to damage, conformability to curved surfaces, and potential for large area distributed actuation and sensing systems. Piezoceramic fibers of small ($\sim 250 \mu\text{m}$) characteristic cross-sectional dimension provide increased specific strength over monolithic materials.

Integral passive materials laminated into the composite, such as glass fibers, can further improve toughness, increasing robustness without compromising the ability to conform to curved shapes. Active fiber composites operate in the longitudinal mode and thus have significantly higher specific work output than planar monolithic piezoceramics. In addition, the directional nature of actuation permits design of modal actuators and sensors without reliance on the host structure to transmit the actuation through structural coupling mechanisms. Large area, multiple ply AFC actuators are easy to fabricate, simplifying leads and connections, and minimizing technology insertion costs.

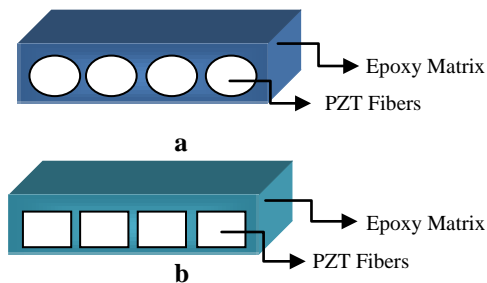


Figure 1: Active Fiber Composite (a), Microfiber Composite (b)

3.2 Microfiber Composite (MFC)

Microfiber Composite is similar to the AFC in the sense that both consist of the same three primary components; active piezoceramic fibers aligned in a unidirectional manner, interdigitated electrodes, and an adhesive polymer matrix, however, the MFC has one difference that greatly affects the manufacturing process and the performance of the actuator, it has rectangular fibers embedded in the polymer matrix Figure 1, b. In addition, MFC results in larger fiber volume contents than the AFC moreover; the maximum fiber volume content of AFC is less than 0.785 because of the restriction in the fiber

geometry. The fiber volume content of MFC could reach up to 0.824. High fiber volume content enhances the performance of the composite and improves the stiffness and strength of the composites. The MFC is extremely flexible, durable and has the advantage of higher Electromechanical coupling coefficients granted through the interdigitated electrodes. Allowing the MFC to be produced at a much lower cost than the AFC and therefore are causing the AFC to be overlooked when determining the ideal actuator for a specific application. Additionally, the rectangular fiber geometry of the MFC guarantees consistent contact between the IDEs and piezoceramic fibers, reducing attenuation on the IDE electric field due to the low dielectric constant of the epoxy matrix. Because of the improved electrical contact, MFC strain performance exceeds AFC strain performance by up to 150%.

4. Shape Control of Composite Laminates

The effect of using several different types of actuators on the behavior of general composite laminates are first studied and compared in order to observe their power to bend the plate enough to counteract any type of external stimuli such as thermal or mechanical deformations. The actuators considered and their properties are summarized in Table 1. The composite laminate is made of Carbon /Epoxy AS4 (3501-6) with symmetric laminates [Actuator/0/60/-60/90]s. The finite elements software COMSOL is used to develop a 3D model in order to predict the response of a simply supported and cantilever composite beam subjected to electric potential difference along the actuators. The finite element mesh is shown in Figure 5. A schematic of the composite beams and the dimensions used is shown in Figure 2.

Figure 3 and Figure 4 show the response of a simply supported and cantilever beam under a 1kN load applied to the midsection and the free end of the composite beam respectively; no voltage was applied to the actuator. The max displacement obtained was 1.2mm and 2mm for both cases respectively. The response of the simply supported composite beam by applying a 200V and 400V electric potential to several different types of actuators is shown in Figure 6 and Figure 7 respectively. Similarly, Figure 9 and Figure 10 present the response of the

cantilever composite beam. The deflection of a typical composite beam is shown in Figure 8.

Table 1: Actuators and composite beam properties

Variable (Unit)	AS4	MFC	AFC	PZT-5H	PZT-4A
E_1 (GPa)	147	30	35	61	60
E_2 (GPa)	10.3	15.5	10.4	61	60
E_3 (GPa)	10.3	15.5	10.4	48	53
ν_{12}	0.27	0.35	0.35	0.31	0.38
ν_{13}	0.27	0.4	0.35	0.31	0.4
ν_{23}	0.54	0.4	0.38	0.31	0.4
G_{12} (GPa)	7	5.7	4.4	23.3	21
G_{13} (GPa)	7	10.7	4.96	19.1	17.3
G_{23} (GPa)	3.7	10.7	4.96	19.1	17.3
d_{31} (pm/V)	-	-198	-260	-274	-171
d_{32} (pm/V)	-	-198	-260	-274	-171
d_{33} (pm/V)	-	418	540	593	374
d_{15} (pm/V)	-	-	-	741	584
d_{24} (pm/V)	-	-	-	741	584
t (mm)	0.3	0.3	0.3	0.3	0.3

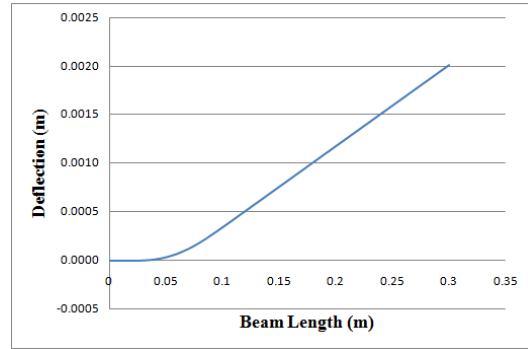


Figure 4: Cantilever composite beam under 1kN load

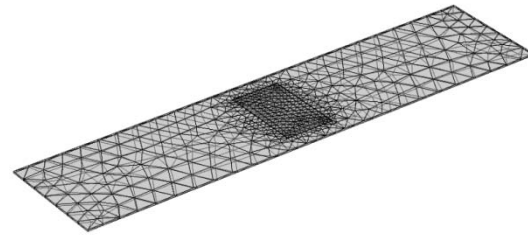


Figure 5: Finite element mesh

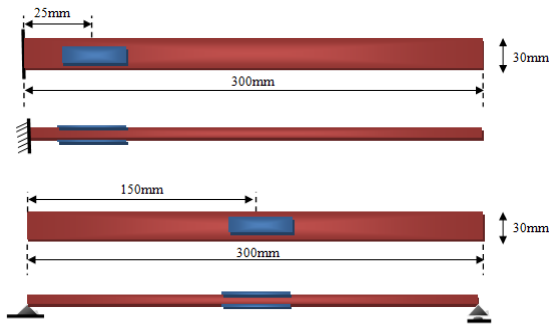


Figure 2: Simply supported and cantilever beam schematics

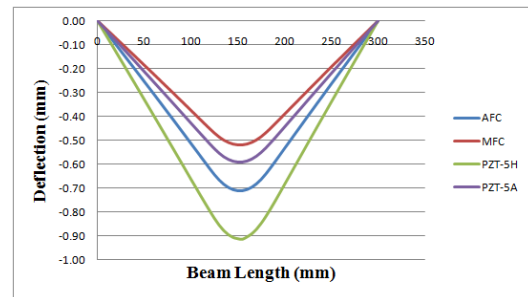


Figure 6: Simply supported beam under 200V electric potential

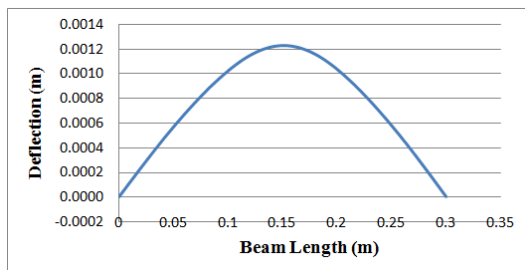


Figure 3: Simply supported composite beam under 1kN load

The piezoelectric fiber composites are actuated through the thickness by using inter digitated electrodes attached to the top and bottom surfaces. The max displacement was obtained by using PZT-5H due to its high piezoelectric coefficient compared to the other actuators. It can be concluded that by using either type of the actuators presented, the deflection caused by the

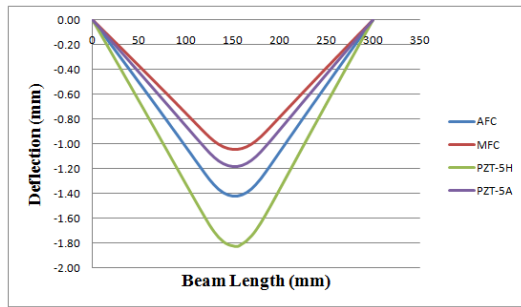


Figure 7: Simply supported beam under 400V electric potential

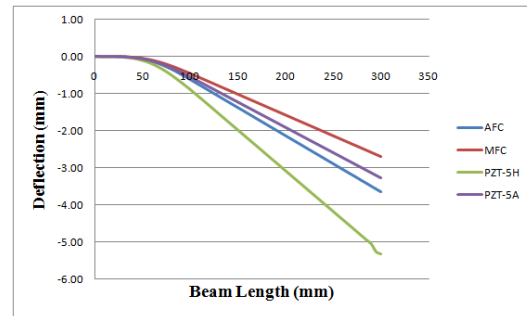


Figure 10: Cantilever beam under 400V electric potential

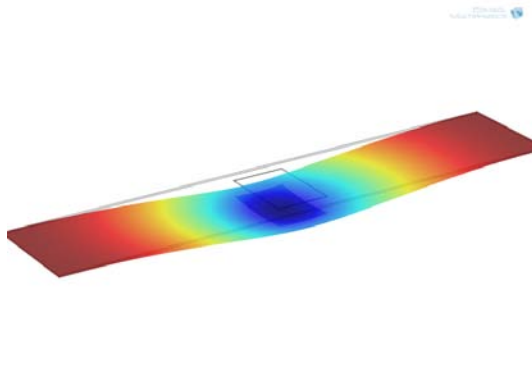


Figure 8: Composite beam deflection under 200V electric potential

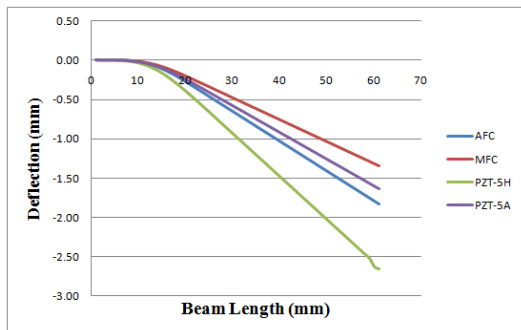


Figure 9: Cantilever beam under 200V electric potential

mechanical load applied to the composite beam can be counter reacted. Also; since all the actuators are suitable in overcoming the deflection of the beam, AFC and MFC have the advantage of having a more flexible behavior in addition to their higher actuation values. It is evident that high stress concentration usually occurs near interfaces of different structures, and in our case, it exists between the host structure

and the active material which might cause delamination of the active part and eventually failure. This type of failure is very common in smart structures. An alternative design could be by using embedded actuators such that, during the manufacturing process, an actuator can be incorporated into the layer by becoming a part of one of the composite layers. This could lead to enhanced behavior of the overall structure and excluding the stress concentration that existed in the previous patched design while obtaining higher actuation values. A comparison between both embedded and patched designs can be shown in Figure 11; it is observed that the embedded design not only excluded the stress concentration, yet, it provided higher actuation values for the same electric potential.

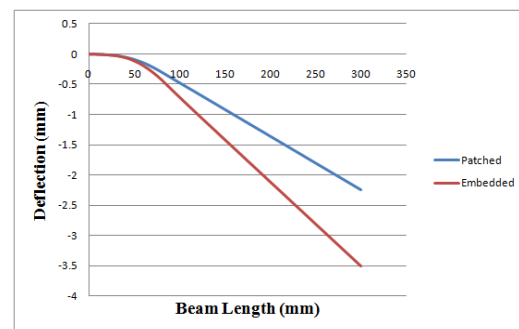


Figure 11: Comparison between patched and embedded actuators on the beam deflection under 200V electric potential

5. Control Design

In most of the industrial applications, structures are usually subjected to several changes such as thermal gradients or mechanical distortions that may affect their overall behavior. Composite structures are usually subjected to

non-uniform temperature change which can induce important thermal distortions. Active control of such structures becomes an essential part of the designing process.

In the present study, we propose a controlling methodology which can be implemented for active controlling of composite structures. The controlling methodology is shown in Figure 12. Based on the results obtained from the first ply failure and ultimate laminate failure of composite structures [12], the control circuit is activated in order to bias the active material with the recommended voltage value to overcome the failure load. Moreover, a control circuit is also implemented using a programmable interfacing chip (PIC) which is programmed and simulated using the simulation program (PROTEOUS). Figure 13 shows a schematic of the control circuit.

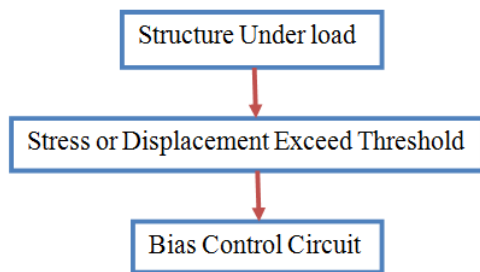


Figure 12: Control methodology

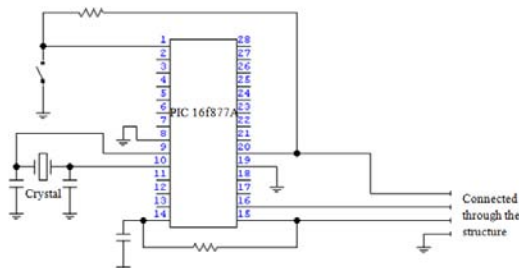


Figure 13: Simple control circuit

6. Conclusion.

The present study focused on the use of piezoelectric material for active control of composite structures. It was observed that the use of piezoelectric fiber composite in smart structures have the advantage of giving higher actuation values yet more flexible structure which give the ability to patch on curved and

bent structures. Due to the high stress concentration between the active material and the host structure which may cause debonding and eventually failure. A proposed design where that active part is incorporated into one of the composite layers, in that way the stress concentration is eliminated and higher deflection is obtained for similar electric potential value. A control methodology was also proposed to control composite structures in order to compensate for any external distortions; in addition, a practical control circuit was implemented using a micro controlling chip (PIC) which showed feasibility in practical use.

7. References

- [1] Gandhi, M.V., Thompson, B. S., "Smart Materials and Structures" Springer, (1992)
- [2] Koconis, D. B., Kollár, L. P. and Springer, G. S., "Shape Control of Composite Plates and Shells with Embedded Actuators" Journal of Composite Materials. 28-5, 459-482, (1994)
- [3] Agrawal, B.N., "Spacecraft vibration suppression using smart structures" 4th Int. Congress on Sound and Vibration, pp 563-70, (1996)
- [4] Lee, C.K., "Theory of laminated piezoelectric plates for the design of distributed sensors/actuators" Part I: governing equations and reciprocal relationships, 144-58, (1990)
- [5] Lee, C. K., "Piezoelectric laminates: theory and experiments for distributed sensors and actuators" Intelligent Structural Systems. Dordrecht: Kluwer, 75-167, (1992)
- [6] Tzou HS, Zhong JP, Hollkamp JJ., "Spatially distributed orthogonal piezoelectric shell actuators: theory and applications" J Sound Vib 363-78, (1994)
- [7] Agrawal, S.K., Tong, D., Nagaraja, K., "Modeling and shape control of piezoelectric actuator embedded elastic plates" J Intelligent Mat Syst Struct 514-22, (1994)
- [8] Atkin, R. Shi, X. Bullough, W., "Solution of the constitutive equations for the flow of an electrorheological fluid" J. Rheol. 35: 1441-1461, (1991)
- [9] Toupin, R.A., "The elastic dielectric" Archives of Rational Mechanics and Analysis 849-915, (1956)
- [10] Knops, R.J., "Two-dimensional electrostriction" Quarterly Journal of Mechanics Applied Mathematics 77-88, (1963)

[11] Reddy, J.N., "Mechanics of laminated plates: theory and analysis" Boca raton, FL: CRC Press, (1997)

[12] Hasan, Z., Darwish, F., "Failure and Stress Analysis of Fiber Reinforced Composite Laminate" AIAA Regional Student Conference, (2010)